

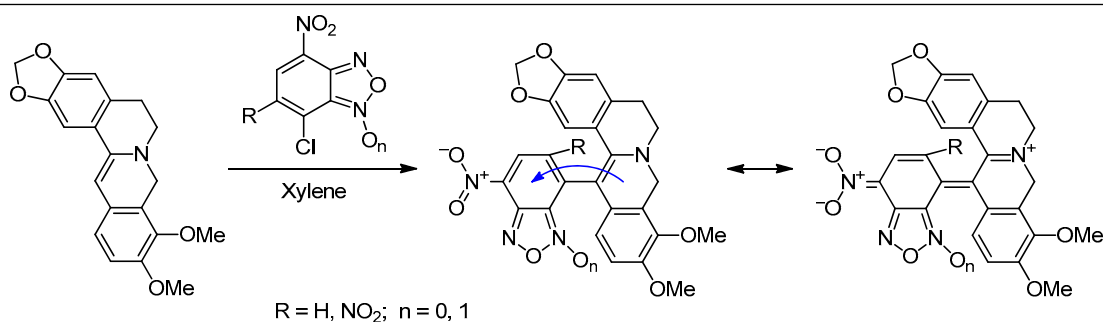
Synthesis and structure of dihydroberberine nitroaryl derivatives – potential ligands for G-quadruplexes

Oleg N. Burov^{1*}, Sergey V. Kurbatov¹, Mikhail E. Kletsii¹,
Alexander D. Zagrebaev¹, Igor E. Mikhailov¹

¹ Southern Federal University,
7 Zorge St., Rostov-on-Don 344090, Russia; e-mail: bboleg@gmail.com

Translated from Khimiya Geterotsiklicheskikh Soedinenii,
2017, 53(3), 335–340

Submitted September 8, 2016
Accepted November 1, 2016



A method was developed for the synthesis of dihydroberberine nitroaryl derivatives on the basis of dihydroberberine reactions with aromatic electrophiles (picryl chloride, 4-chloro-7-nitrobenzofurazan, 4-chloro-5,7-dinitrobenzofurazan, and 7-chloro-4,6-dinitrobenzofuroxan). The obtained 13-substituted dihydroberberine derivatives represent structures with significant intramolecular charge transfer and, according to the results of molecular docking analysis, can effectively bind with G-quadruplexes of telomeric DNA fragments.

Keywords: berberine, dihydroberberine, 4,6-dinitrobenzofurazan, 4,6-dinitrobenzofuroxan, G-quadruplex, molecular docking, nucleophilic aromatic substitution, DFT calculations.

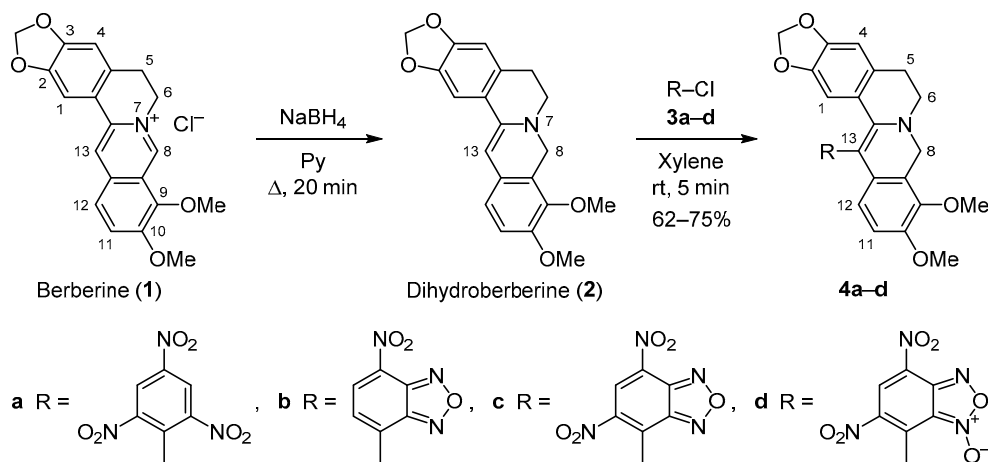
Berberine (**1**) and its derivatives exhibit a broad range of biological activity, which has been described in review articles^{1,2} and continues to motivate further research in the areas of organic synthesis and medicinal chemistry toward developing new routes for structural modification of this alkaloid. In our opinion, one of the most attractive areas for the application of berberine derivatives relies on their ability to bind with G-quadruplexes found in telomeric regions of DNA,³ which provide universal biological targets in systemic therapy of oncological diseases.^{4,5} The formation of noncovalent complexes with G-quadruplexes in promoter regions of oncogenes, as well as in telomeric regions of chromosomes in combination with telomerase inhibition provides opportunities for blocking uncontrolled division of cancer cells and leads to their apoptosis.⁶ G-quadruplexes are a specific secondary structure type observed in DNA regions that are enriched in deoxyguanosine and are composed of four coplanar guanine bases. These guanine bases are stabilized by hydrogen bonds in a way that the oxygen atoms of guanine

carbonyl groups can additionally interact with planar organic cations and/or Lewis acids.⁷

Berberine derivatives have significant affinity for various types of G-quadruplexes due to the presence of positively charged extended π -system in their molecules.^{3,7} Berberines, similarly to other planar polycondensed heterocyclic systems, form intercalation complexes with G-quadruplexes,⁸ which are stabilized by hydrophobic, ionic, and van der Waals interactions. More distant, non-specific binding between anionic or neutral ligands and DNA is also possible, mediated by electrostatic interactions (including *via* hydrogen bonds) of the ligand with the sugar-phosphate backbone of DNA.

Analysis of the main types of coordination between small molecules and G-quadruplexes led to the known requirements for the structure of potential ligands, which have been presented in review articles.^{9,10} First, the molecule of potential ligand must contain planar polycondensed cyclic structures, capable of stacking. Second, it is desirable to have additional charged groups able of

Scheme 1



forming complexes not only by intercalation, but also by ionic interactions.

The goal of this work was to synthesize and study nitroaryl derivatives of berberine, with structures that satisfy these requirements and feature significant intramolecular charge transfer, offering possibilities for additional polar interactions. The great value of nitroarylation of berberine derivatives that contain enamine moiety was demonstrated previously for acetylberberine.¹¹ However, this method did not allow us to obtain planar structures necessary for binding with G-quadruplexes.

In this work, we report the first use of dihydroberberine (2) as a substrate for the introduction of nitroaryl substituents at position 13. Our selected arylating reagents were highly electrophilic chloronitroarenes: picryl chloride (3a), 4-chloro-7-nitrobenzofurazan (3b), 4-chloro-5,7-dinitrobenzofurazan (3c), and 7-chloro-4,6-dinitrobenzofuroxan (3d) (Scheme 1). The reduction of berberine chloride (1) to dihydroberberine (2) was performed according to a previously described procedure.¹²

The reactions of dihydroberberine (2) with equivalent amounts of chloronitroarenes 3a–d were performed in xylene at room temperature. This led to rapid formation of dihydroberberine 13-nitroaryl derivatives 4a–d in the form of deeply colored crystals (Scheme 1). The selection of xylene as reaction medium was based on the good solubility of the starting compounds and reaction by-products in this solvent. The target products formed precipitates that were relatively pure.

Our previously synthesized diaryls of similar type, containing both electron-donating and highly electrophilic moieties, showed significant intramolecular charge transfer through a conjugated system of chemical bonds.^{13,14} The substantial contribution of resonance structures of type 4a–d in the electron density distribution was experimentally demonstrated by the chemical shifts of signals due to protons located next to the berberine nitrogen atom (Table 1, Fig. 1). It should be noted that structural characterization of nitrogen-containing compounds requires not only ¹H NMR spectra, but also ¹⁵N NMR spectra, which can be highly important.¹⁵ However, taking into account the particular

importance of ¹H NMR data for the majority of chemists, as well as the reliability of information thus obtained about the chemical shifts of protons located near the cationic center, in this work we relied on ¹H NMR spectroscopy.

In order to determine the contribution of bipolar component in the structures of the obtained compounds 4a–d, we performed a computational study within the framework of density functional theory, using the B3LYP exchange-correlation functional with 6-31G** basis set. This level of approximation has been found to be adequate for evaluating the electronic and geometry characteristics of nitro derivatives of oxazoles¹⁴ and berberines.¹⁶

The most significant parameters that we selected for evaluating the contribution of bipolar structures were intramolecular charge transfer to the nitroaryl group, the bond length between berberine and nitroaryl groups, and the rotation angle of the nitroaryl substituent relative to the plane of berberine ring system (Table 1).

The selected criterion for evaluating the extent of charge transfer was the total Mulliken charge on the nitroaryl (berberine) moiety of compounds 4a–d. As shown in Table 1, there is a significant charge transfer in compounds 4a–d in the direction from dihydroberberine ring system to the nitroaryl group (Fig. 1). Besides that, the significant charge transfer in the aforementioned direction was evidenced also

Table 1. The chemical shifts of characteristic protons and the main physical characteristics of compounds 4a–d according to calculations using the B3LYP method with 6-31G** basis set

Parameter	Compound			
	4a	4b	4c	4d
Chemical shift of 6-CH ₂ , δ, ppm	3.18	3.26	4.05–4.12 4.30–4.37	4.12–4.17 4.98–5.04
Chemical shift of 8-CH ₂ , δ, ppm	4.55	4.62	4.97–5.14	5.32–5.37
Charge transfer, e ⁻	0.254	0.304	0.398	0.425
Dipole moment, D	4.56	8.72	8.26	8.38
Length of C(13)–C(7') bond, Å*	1.480	1.471	1.461	1.460
Dihedral angle C(12')–C(13)–C(7')–C(6'), deg.**	72	54	55	57

* The length of C(13)–C(1') bond is given for compound 4a.

** The dihedral angle C(12)–C(13)–C(1')–C(2) is given for compound 4a.

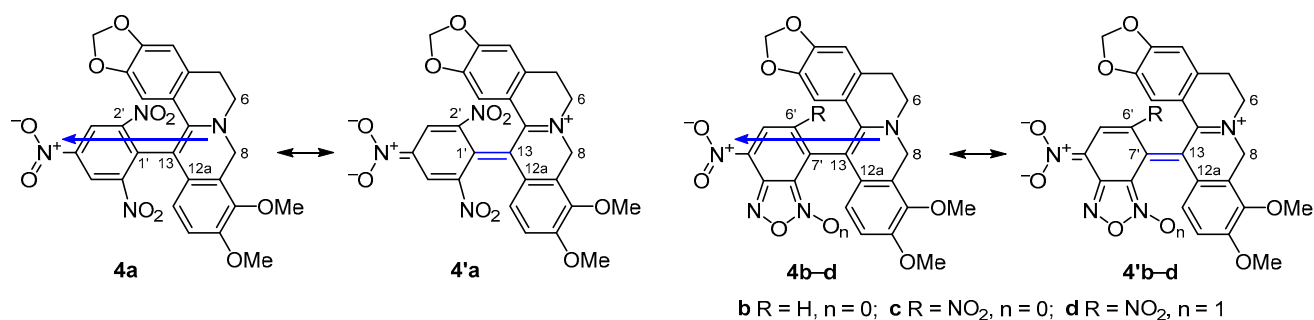


Figure 1. The direction of dipole moment (charge transfer) and the possible resonance structures of compounds **4a–d**.

by the calculated dipole moments of compounds **4a–d** (Table 1, the directions of dipole moments are shown in Fig. 1). The increasing extent of charge transfer in compounds **4a–d** from berberine moiety to the nitroaryl group is apparently associated with increased contribution of resonance structures **4'a–d** with separated charges.

The negative charge in the nitroaryl moiety was mostly concentrated on the oxygen atoms of nitro groups. As shown in Figure 2, the carbon skeleton of the nitroaryl moiety in compounds **4b–d** was positively charged, similarly to the berberine ring system.

In the case of compounds **4a–d**, the significant charge transfer correlated with changes in ¹H NMR chemical shift of 6-CH₂ and 8-CH₂ protons which were the closest to the N-7 nitrogen atom (Table 1). This observation also pointed to the substantial contribution of structures with separated charges. The downfield ¹H NMR shift for the protons located in the cationic part of the molecule is often used to estimate the extent of charge transfer in bipolar spirocycles^{17,18} and intramolecular π -complexes.¹⁹

Compounds **4a–d** belong to the class of pseudo-cross-conjugated systems,²⁰ as evidenced by the results of our quantum-chemical calculations. Thus, the negatively charged nitroaryl fragment is rotated relatively to the positively charged berberine ring system by 54–72° (Table 1). It is interesting to note that the length of the C(13)–C(7') bond (C(13)–C(1') in compound **4a**), according to the calculations, is intermediate between that of ordinary and double bonds. At the same time, the length of bond between the nitroaryl and berberine moieties correlates with the extent of charge transfer.

It is interesting to note that the C(13)–C(7') bond, formed as a result of the discussed reactions, is activated with respect to both electrophilic and nucleophilic attack. The calculation of Parr's indices²¹ showed that this bond is strongly polarized: the maximum index of electrophilicity f_k^+ corresponded to the C(7') atom of compounds **4b–d** (C(1') atom of compound **4a**), while the maximum index of nucleophilicity f_k^- was found on the C(13) atom of berberine fragment. The aforementioned findings mean that the significant non-coplanarity of compounds **4a–d** (Table 1) makes the C(13)–C(7') bond highly active in addition reactions. This fact can be quite useful for the formation of weak associative bonds with enzymes or nucleic acid fragments.

Molecular docking of compounds 4a–d. Nucleic acid regions capable of G-quadruplex formation create obstacles for DNA synthesis by polymerases and reverse transcriptases.²² It has been shown *ex vivo* that quadruplexes cause apoptosis in tumor cells.²³ Ligands that stabilize DNA quadruplexes in oncogen promoter regions can suppress their hyperexpression.²⁴ Deactivation of oncogenes deprives the cell of proteins associated with the pathological process.²⁵ As noted above, the structures with intramolecular charge transfer on the basis of berberine may serve as promising ligands for binding with G-quadruplexes. In order to confirm this hypothesis, we performed modeling of docking processes between compounds **4a–d** and some G-quadruplexes from the G4LDB database.⁷ We selected as targets such types of quadruplexes as **3QSC**, **3MIJ**, and **2JWQ**.

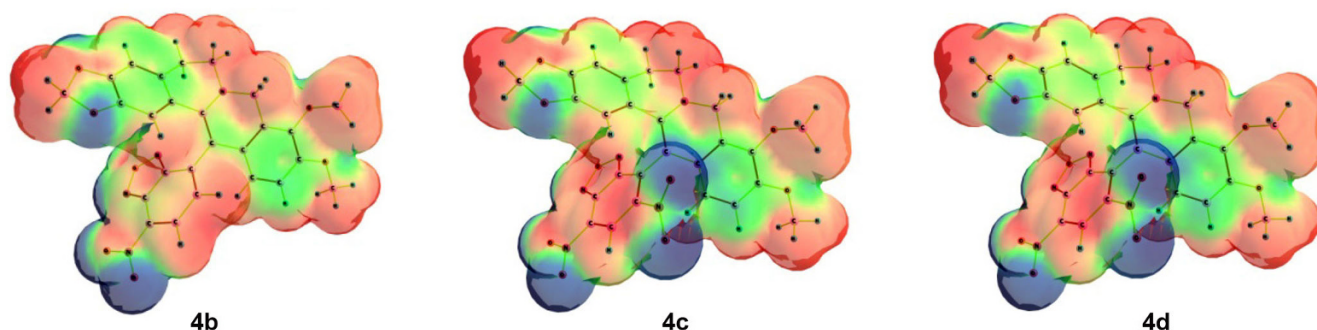


Figure 2. Electrostatic potential surfaces of oxadiazoles **4b–d**. The areas of maximum negative potential are marked in blue, while the areas of maximum positive potential are red.

The sequence **2JWQ**²⁶ represents a DNA fragment d[T₂AG₃], composed of three aggregated G-tetrads, connected by loops with different spatial configuration.^{27–29}

The sequence **3QSC**³⁰ represents a DNA fragment d(AG₃TUAG₃T₂), also composed of three aggregated G-tetrads. The sequence **3MIJ**³¹ represents a RNA fragment r(UAG₃U₂AG₃U), capable of forming two-chain associates.

It was established that molecules which interacted with any of the first two tetrads, stabilizing the quadruplex structure, led to telomere dysfunction due to disruption of telomere-protein interactions^{32,33} and, in particular, altered the binding with telomerase. The compounds that formed complexes with the structure of **3MIJ** also caused inhibition of telomerase. It is known that telomerase is a key enzyme for proliferation of cancer cells, as it is involved in the process of their immortalization by preventing the normal process of telomere shortening. Remarkably, this enzyme is active in the majority of cancer cells (85%) and shows little or no activity in healthy somatic cells.^{34,35}

The effectiveness of interaction between ligand and G-quadruplex was expressed by using the widely accepted pK_i value as criterion, which is equal to the negative decimal logarithm of "inhibition" constant K_i , representing a ratio between the product of ligand and G-quadruplex concentrations and the concentration of the formed complex. Generalization of the experimental results allowed to formalize the requirements to the characteristics of potential quadruplex ligands. Promising ligands of G-quadruplexes must exhibit high affinity for G-quadruplex and a good "quadruplex/duplex" selectivity (the ligand binding constant with G-quadruplex ($1/K_i$) must not be lower than 10^6 M^{-1} , therefore $pK_i \geq 6$).³⁶

The zwitterionic berberine derivatives **4a–d** showed the highest affinity for DNA quadruplexes upon complex formation by intercalation mechanism (Table 2, Fig. 3).

The strongest binding of compounds **4a–d** occurred with loose G-quadruplexes of telomerases that were formed by

Table 2. The inhibition constants (pK_i) for several G-quadruplexes by compounds **4a–d** according to the docking models

G-quadruplex*	Compound			
	4a	4b	4c	4d
3QSC	6.62	7.08	7.75	8.68
3MIJ	4.91	4.83	5.09	5.23
2JWQ	6.54	0.21	6.57	7.21

* The abbreviations are given according to the protein database (PDB ID).

several DNA strands (Fig. 3). It is interesting to note that the activity in series of oxadiazoles **4b–d** was directly dependent on the extent of intramolecular charge transfer. At the same time, in the case of some G-quadruplexes compound **4a** gave larger pK_i values compared to compound **4b**, although there is a higher degree of charge transfer in the latter molecule. This observation can be explained by the less planar structure of compound **4a**, which interacts more readily with DNA fragments.

The strongest binding in docking was observed between compound **4d** and sequence **3QSC** (Table 2, Fig. 3). As shown in Figure 3, the dinitrofurazan derivative **4d** formed an intercalation complex, in which the berberine ring system was located between two loops of nucleic acid and was coordinated with four guanine residues. The nitroaryl group in this complex was rotated at a significant angle relative to the berberine skeleton and formed two additional hydrogen bonds with NH groups of thymine residues.

Obtained molecular docking results showed that the significant intramolecular charge transfer in berberine derivatives can lead to the formation of stable inclusion complexes with G-quadruplexes, which are additionally stabilized by binding between the anionic part of the molecule and the non-guanine fragments of quadruplexes.

Thus, we have developed a method for the modification of berberine molecule by introducing highly electrophilic aromatic substituents through the formation of a new

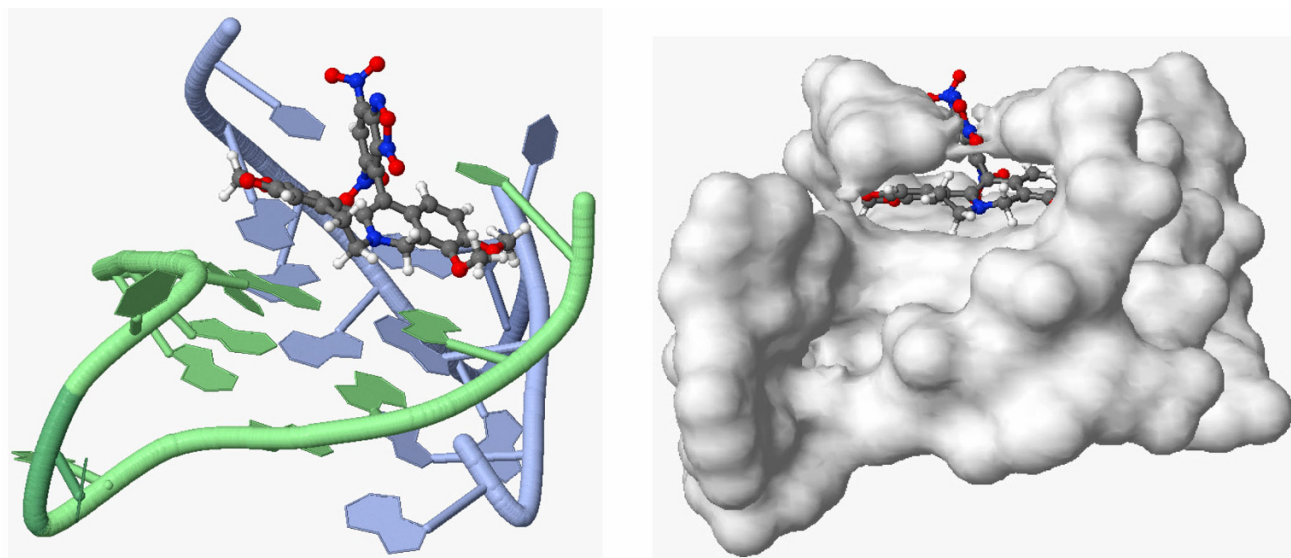


Figure 3. A complex of compound **4d** and G-quadruplex **3QSC** with symbolic representation of DNA (left) and taking into account the van der Waals radii in quadruplex (right), according to the results obtained from online modeling service g4ldb.com.⁷

carbon–carbon bond at position 13. According to quantum-chemical calculations, the obtained compounds are characterized by a high degree of intramolecular charge transfer and, according to molecular docking models, can be used as promising ligands for G-quadruplexes in telomeric DNA fragments. The presence of a planar electron-withdrawing moiety can enable the coordination with additional binding sites of DNA molecules.

Experimental

¹H and ¹³C NMR spectra were acquired on a Bruker DPX-250 instrument (250 and 63 MHz, respectively), with TMS as internal standard. The assignment of ¹H NMR signals was confirmed on the basis of two-dimensional COSY and NOESY NMR experiments. An overlap of several ¹³C NMR signals was observed, reducing their number to less than theoretically expected. High-resolution mass spectra were recorded on a Bruker micrOTOF II instrument (electrospray ionization). Ion signals were measured in positive ion mode (capillary voltage 4500 V). The mass scanning range was 50–3000 Da. Decomposition temperatures were determined in glass capillaries, using a PTP apparatus. Column chromatography was performed with Merck Silicagel 60 (70–230 μm). Commercially available berberine chloride hydrate (**1**) (Alfa Aesar) and 4-chloro-7-nitrobenzofurazan (**3b**) (Alfa Aesar) were used in the syntheses. Dihydroberberine (**2**),¹² picryl chloride (**3a**),³⁷ 4-chloro-5,7-dinitrobenzofurazan (**3c**),³⁸ and 7-chloro-4,6-dinitrobenzofuroxan (**3d**)³⁹ were synthesized according to published procedures.

Synthesis of nitroaryl derivatives 4a–d (General method). A solution of the appropriate chloronitroarene **3a–d** (1.0 mmol) in xylene (10 ml) was added to a solution of dihydroberberine (**2**) (337 mg, 1.0 mmol) in xylene (15 ml). The reaction mixture was stirred for 5 min at room temperature, the precipitate that formed was filtered off, dried, and separated by chromatography on silica gel (eluent CHCl₃–EtOH, 10:1). The obtained compounds **4a–d** were recrystallized from isopropanol.

13-(2,4,6-Trinitrophenyl)-7,8-dihydroberberine (4a). Yield 412 mg (75%), dark-green needle-shaped crystals, decomp. temp. >157°C. ¹H NMR spectrum (CDCl₃), δ, ppm (*J*, Hz): 2.78 (2H, t, *J* = 7.5, 5-CH₂); 3.18 (2H, t, *J* = 7.5, 6-CH₂); 3.82 (3H, s, 10-OCH₃); 3.88 (3H, s, 9-OCH₃); 4.55 (2H, s, 8-CH₂); 5.89 (2H, s, OCH₂O); 6.07 (1H, d, *J* = 8.6, H-12); 6.20 (1H, s, H-1); 6.61 (1H, d, *J* = 8.6, H-11); 6.65 (1H, s, H-4); 8.72 (2H, s, H-3',5'). ¹³C NMR spectrum (CDCl₃), δ, ppm: 31.0; 48.1; 49.2; 55.8; 60.8; 98.1; 101.3; 107.5; 108.3; 111.1; 116.2; 122.3; 123.0; 123.1; 126.6; 133.2; 136.4; 142.7; 144.3; 145.6; 145.9; 148.2; 151.3; 152.7. Found, *m/z*: 547.1090 [M–H]⁺. C₂₆H₂₀N₄O₁₀. Calculated, *m/z*: 547.1096.

13-(7-Nitrobenzofurazan-4-yl)-7,8-dihydroberberine (4b). Yield 339 mg (68%), dark-green needle-shaped crystals, decomp. temp. >130°C. ¹H NMR spectrum (CDCl₃), δ, ppm (*J*, Hz): 2.93 (2H, t, *J* = 5.6, 5-CH₂); 3.26 (2H, t, *J* = 5.7, 6-CH₂); 3.81 (3H, s, 10-OCH₃); 3.87 (3H, s, 9-OCH₃); 4.62 (2H, s, 8-CH₂); 5.76 (2H, s, OCH₂O); 6.14 (1H, s, H-1); 6.35 (1H, d, *J* = 8.6, H-12); 6.60 (1H, s, H-4); 6.62 (1H, d,

J = 8.7, H-11); 7.39 (2H, d, *J* = 7.8, H-5'); 8.43 (2H, d, *J* = 7.8, H-6'). ¹³C NMR spectrum (DMSO-*d*₆), δ, ppm: 26.6; 49.0; 52.0; 55.4; 61.2; 103.1; 109.1; 109.3; 112.0; 115.7; 116.8; 117.8; 121.5; 124.0 (2C); 126.3; 126.6; 132.8; 135.7; 145.0; 146.5; 146.7; 149.2 (2C); 153.8; 170.0. Found, *m/z*: 499.1241 [M–H]⁺. C₂₆H₂₀N₄O₇. Calculated, *m/z*: 499.1248.

13-(5,7-Dinitrobenzofurazan-4-yl)-7,8-dihydroberberine (4c). Yield 397 mg (73%), dark-violet needle-shaped crystals, decomp. temp. >119°C. ¹H NMR spectrum (DMSO-*d*₆), δ, ppm (*J*, Hz): 3.07–3.16 (2H, m, 5-CH₂); 3.83 (3H, s, 10-OCH₃); 3.86 (3H, s, 9-OCH₃); 4.05–4.12 (1H, m) and 4.30–4.37 (1H, m, 6-CH₂); 4.97–5.14 (2H, m, 8-CH₂); 6.09 (1H, s) and 6.24 (1H, s, OCH₂O); 7.09 (1H, d, *J* = 8.8, H-11); 7.13 (1H, s, H-4); 7.56 (1H, d, *J* = 8.7, H-12); 7.60 (1H, s, H-1); 8.59 (1H, s, H-6'). ¹³C NMR spectrum (DMSO-*d*₆), δ, ppm: 26.4; 49.1; 52.6; 56.5; 61.5; 103.2; 109.8; 110.4; 112.7; 115.9; 117.1; 117.6; 121.7; 124.2; 124.5; 126.4; 127.2; 132.9; 135.6; 145.0; 146.5; 147.5; 149.7; 152.2; 153.9; 170.0. Found, *m/z*: 544.1108 [M–H]⁺. C₂₆H₁₉N₅O₉. Calculated, *m/z*: 544.1099.

13-(5,7-Dinitrobenzofuroxan-4-yl)-7,8-dihydroberberine (4d). Yield 347 mg (62%), red needle-shaped crystals, decomp. temp. >104°C. ¹H NMR spectrum (CDCl₃), δ, ppm (*J*, Hz): 3.37–3.42 (2H, m, 5-CH₂); 4.12–4.17 (1H, m) and 4.98–5.04 (1H, m, 6-CH₂); 5.20 (3H, s, 10-OCH₃); 5.24 (3H, s, 9-OCH₃); 5.32–5.37 (2H, m, 8-CH₂); 6.68 (2H, s, OCH₂O); 7.47 (1H, s, H-4); 8.18 (1H, d, *J* = 8.9, H-11); 8.36 (1H, d, *J* = 8.9, H-12); 8.73 (1H, s, H-1); 10.17 (1H, s, H-6'). ¹³C NMR spectrum (pyridine-*d*₅), δ, ppm: 29.5; 43.5; 45.3; 57.1; 61.8; 103.2; 108.6; 109.6; 112.1; 128.0; 130.9; 131.7; 133.9; 135.8; 137.4; 148.3; 156.9; 165.5. Found, *m/z*: 562.1188 [M+H]⁺. C₂₆H₁₉N₅O₁₀. Calculated, *m/z*: 562.1205.

Computational method. Quantum-chemical calculations were performed for molecules in gas phase within the framework of the density functional theory using 6-31G** basis set and B3LYP functional, including Becke three-parameter exchange functional and Lee–Yang–Parr correlation functional.^{40,41} The global electrophilicity indices ω were calculated according to the scheme proposed by Parr.²¹ This was achieved by using the energy of highest occupied (ε_H) and lowest unoccupied (ε_L) molecular orbitals in the ground state: ω = μ²/2η, where μ = (ε_H + ε_L)/2, η = ε_L – ε_H. Molecular docking was modeled by using the online service at g4ldb.com.⁷

This study was supported by a grant from the Russian Science Foundation (project 14-13-00103).

References

1. Nechepurenko, I. V.; Salakhutdinov, N. F.; Tolstikov, G. A. *Khimiya v Interesakh Ustoichivogo Razvitiya* **2010**, 18, 1.
2. Grycová, L.; Dostál, J.; Marek, R. *Phytochemistry* **2007**, 68, 150.
3. Zhang, W.-J.; Ou, T.-M.; Lu, Y.-J.; Huang, Y.-Y.; Wu, W.-B.; Huang, Z.-S.; Zhou, J.-L.; Wong, K.-Y.; Gu, L.-Q. *Bioorg. Med. Chem.* **2007**, 15, 5493.
4. Balasubramanian, S.; Hurley, L. H.; Neidle S. *Nat. Rev. Drug Discovery* **2011**, 10, 261.

5. De Cian, A.; Lacroix, L.; Douarre, C.; Temime-Smaali, N.; Trentesaux, C.; Riou, J. F.; Mergny, J. L. *Biochimie* **2008**, *90*, 131.
6. Cavallari, M.; Garbesi, A.; Di Felice, R. *J. Phys. Chem. B* **2009**, *113*, 13152.
7. Li, Q.; Xiang, J.-F.; Yang, Q.-F.; Sun, H.-X.; Guan, A.-J.; Tang, Y.-L. *Nucleic Acids Res.* **2013**, *41*, D1115.
8. Jiménez-Banzo, A.; Sagristà, M. L.; Mora, M.; Nonell, S. *Free Radical Biol. Med.* **2008**, *44*, 1926.
9. Xiong, Y.-X.; Huang, Z.-S.; Tan, J.-H. *Eur. J. Med. Chem.* **2015**, *97*, 538.
10. Bhadra, K.; Kumar, G. S. *Biochim. Biophys. Acta* **2011**, *1810*, 485.
11. Burov, O. N.; Kurbatov, S. V.; Morozov, P. G.; Kletskii, M. E.; Tatarov, A. V. *Chem. Heterocycl. Compd.* **2015**, *51*, 772. [*Khim. Geterotsikl. Soedin.* **2015**, *51*, 772.]
12. Lyamzaev, K. G.; Pustovidko, A. V.; Simonyan, R. A.; Rokitskaya, T. I.; Domnina, L. V.; Ivanova O. Y.; Severina, I. I.; Sumbatyan, N. V.; Korshunova, G. A.; Tashlitsky, V. N.; Roginsky, V. A.; Antonenko, Y. N.; Skulachev, M. V.; Chernyak, B. V.; Skulachev, V. P. *Pharm. Res.* **2011**, *28*, 2883.
13. Kurbatov, S.; Tatarov, A.; Minkin, V.; Goumont, R.; Terrier, F. *Chem. Commun.* **2006**, 4279.
14. Semenyuk, Yu. P.; Kochubei, A. S.; Morozov, P. G.; Burov, O. N.; Kletskii, M. E.; Kurbatov, S. V. *Chem. Heterocycl. Compd.* **2014**, *50*, 1731. [*Khim. Geterotsikl. Soedin.* **2014**, 1881.]
15. Larina, L. I.; Lopyrev, V. A. *Nitroazoles: Synthesis, Structure and Applications*; Springer: New York, 2009, 446 p.
16. Burov, O. N.; Kletskii, M. E.; Fedik, N. S.; Kurbatov, S. V.; Lisovin, A. V. *Chem. Heterocycl. Compd.* **2015**, *51*, 997. [*Khim. Geterotsikl. Soedin.* **2015**, *51*, 997.]
17. Tkachuk, A. V.; Samarin, K. A.; Kletskii, M. E.; Burov, O. N.; Golikov, A. Yu.; Kurbatov, S. V.; Minkin, V. I. *Rus. J. Org. Chem.* **2014**, *50*, 1223. [*Zh. Org. Khim.* **2014**, *50*, 1237.]
18. Tkachuk, A. V.; Kurbatov, S. V.; Burov, O. N.; Kletskii, M. E.; Morozov, P. G.; Minkin, V. I. *Chem. Heterocycl. Compd.* **2014**, *50*, 26. [*Khim. Geterotsikl. Soedin.* **2014**, 32.]
19. Minkin, V. I.; Tkachuk, A. V.; Kletskii, M. E.; Steglenko, D. V.; Voronina, V. A.; Kurbatov, S. V. *Rus. Chem. Bull., Int. Ed.* **2013**, *62*, 464. [*Izv. Akad. Nauk, Ser. Khim.* **2013**, 464.]
20. Ramsden, C. A. *Tetrahedron* **2013**, *69*, 4146.
21. Parr, R. G.; Szentpály, L.V.; Liu, S. *J. Am. Chem. Soc.* **1999**, *121*, 1922.
22. Woodford, K. J.; Howell, R. M.; Usdin, K. *J. Biol. Chem.* **1994**, *269*, 27029.
23. Qi, H.; Lin, C.-P.; Fu, X.; Wood, L. M.; Liu, A. A.; Tsai, Y.-C.; Chen, Y.; Barbieri, C. M.; Pilch, D. S.; Liu, L. F. *Cancer Res.* **2006**, *66*, 11808.
24. Hurlley, L. H. *Nat. Rev. Cancer* **2002**, *2*, 188.
25. Weinstein, I. B.; Joe, A. K. *Nat. Clin. Pract. Oncol.* **2006**, *3*, 448.
26. Hounsou, C.; Guittat, L.; Monchaud, D.; Jourdan, M.; Saettel, N.; Mergny, J.-L.; Teulade-Fichou, M.-P. *ChemMedChem* **2007**, *2*, 655.
27. Burge, S.; Parkinson, G. N.; Hazel, P.; Todd, A. K.; Neidle, S. *Nucleic Acids Res.* **2006**, *34*, 5402.
28. Phan, A. T.; Kuryavyi, V.; Patel, D. J. *Curr. Opin. Struct. Biol.* **2006**, *16*, 288.
29. Davis, J. T. *Angew. Chem., Int. Ed.* **2004**, *43*, 668.
30. Campbell, N. H.; Abd Karim, N. H.; Parkinson, G. N.; Gunaratnam, M.; Petrucci, V.; Todd, A. K.; Vilar, R.; Neidle, S. *J. Med. Chem.* **2012**, *55*(1), 209.
31. Collie, G. W.; Sparapani, S.; Parkinson, G. N.; Neidle, S. *J. Am. Chem. Soc.* **2011**, *133*, 2721.
32. Gomez, D.; Aouali, N.; Londoño-Vallejo, A.; Lacroix, L.; Mégnin-Chanet, F.; Lemarteleur, T.; Douarre, C.; Shin-ya, K.; Mailliet, P.; Trentesaux, C.; Morjani, H.; Mergny, J.-L.; Riou, J.-F. *J. Biol. Chem.* **2003**, *278*, 50554.
33. Burger, A. M.; Dai, F.; Schultes, C. M.; Reszka, A. P.; Moore, M. J.; Double, J. A.; Neidle, S. *Cancer Res.* **2005**, *65*, 1489.
34. Kim, N. W.; Piatyszek, M. A.; Prowse, K. R.; Harley, C. B.; West, M. D.; Ho, P. L.; Coviello, G. M.; Wright, W. E.; Weinrich, S. L.; Shay, J. W. *Science* **1994**, *266*, 2011.
35. Shay, J. W.; Bacchetti, S. *Eur. J. Cancer* **1997**, *33*, 787.
36. Neidle, S. *FEBS J.* **2010**, *277*, 1118.
37. Boyer, R.; Spencer, E. Y.; Wright, G. F. *Can. J. Res.* **1946**, *24B*, 200.
38. Norris, W. P.; Chafin, A.; Spear, R. J.; Read, R. W. *Heterocycles* **1984**, *22*, 271.
39. Sharnin, G. P.; Levinson, F. S.; Akimova, S. A.; Khasanov, R. Kh. USSR Author's Certificate 627129; *Byul. Izobret.* **1978**, (37).
40. Becke, A. D. *Phys. Rev. A* **1988**, *38*, 3098.
41. Becke, A. D. *J. Chem. Phys.* **1993**, *98*, 5648.